Construction and Building Materials 400 (2023) 132610

Contents lists available at ScienceDirect

Construction and Building Materials

journal homepage: www.elsevier.com/locate/conbuildmat

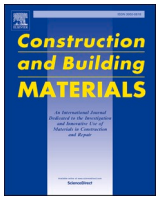

A high-performance rubberised alkali-activated mortar for repair of RC beams

Amin Zakeremamreza, Mohammad E. Kianifar, Chidera Chibuisi, Ehsan Ahmadi *, Mohammad R. Salami

School of Engineering and the Built Environment, Birmingham City University, UK

ARTICLE INFO

Keywords:
Waste tire rubber alkali-activated mortar
RC concrete beams
Concrete repair
Flexural strength
Compressive strength
Bonding strength, water absorption

ABSTRACT

The application of recycled waste tyre rubber in construction materials is increasingly growing due to its economic, environmental, and technical benefits. This study, in particular, examines the potential use of a waste tire rubber alkali-activated mortar in effective repair of damaged RC beams, which contains a very slight embodied-carbon footprint compared to the existing repair mortars. To assess the effectiveness of the proposed mortar for repair purposes, an extensive set of small-scale mortar samples with diverse contents are designed, assembled, and tested for compressive strength, flexural strength, bonding strength, and water absorption capacity. After discovering the efficient mortar mix that in general provides improved performance, large-scale RC beams are designed, constructed, damaged, repaired, and tested in flexure. It is found that the proposed mortar showed remarkable results and potential as a repair material. It contains significantly lower embodied carbon (35.3 kg/m^3) compared to ordinary mortar (530.8 kg/m^3). Also, the beam repaired by the proposed mortar exhibits high overall performance including strength capacity, ductility index, and bonding feature that are superior to the existing mortars. In particular, the experimental results demonstrated about 20 % increase in cracking load and 30 % increase in maximum displacement compared to the undamaged beam.

1. Introduction

1.1. Background

Concrete is one of the most popular materials in the construction sector, where ageing of reinforced concrete (RC) structures is a major issue. Even though millions of RC structures are globally built each year, such structures deteriorate and become unsafe and less durable due to a wide range of environmental-operational factors (e.g., chemical attacks, corrosion, overloading, fatigue, usage change, etc.) [1]. More specifically, time-varying decay of concrete's mechanical properties leads to time-dependent deteriorations (e.g., creep and shrinkage), and the exposure of the cracked concrete —due to overloading and fatigue— to harsh environmental conditions (e.g., sulphate and chloride) results in concrete cover spalling, reinforcement corrosion, and consequently, the loss of structural serviceability and longevity, safety, and resilience [2–4]. It is reported that more than 3,200 RC bridges in the UK are rated as damaged [5], and almost half the highway bridges have structural components with a poor or very poor condition [6].

As environmental-operational factors reduce concrete's lifecycle, regular repair and maintenance of RC structures are essential for improved durability and safety [7,8]. As such, a gradual rise in repair works is seen due to ageing RC structures. The repair of RC structures is very cost-effective and inappropriate repair materials might lead to a never-ending cycle of repair works due to incompatibility of the repair material with the concrete substrate [3,9–11]. An appropriate repair material must result in a strongly bonded and durable repair and at least provide strength and ductility capacities similar to the undamaged component [3,12,13]. In certain cases, it could be more cost effective to accept the need for repair at appropriate intervals rather than try to construct a new replacement structure that will remain maintenance-free for a considerable amount of time in harsh circumstances. Hence, the construction industry growingly demands for sustainable repair materials to ensure public safety, continued serviceability of RC infrastructure, and eco-friendly and cost-effective repair means.

* Corresponding author.
E-mail address: ehsan.ahmadi@bcu.ac.uk (E. Ahmadi).

https://doi.org/10.1016/j.conbuildmat.2023.132610
Received 29 May 2023; Received in revised form 18 July 2023; Accepted 24 July 2023
Available online 28 July 2023

1.2. Existing repair materials

A wide variety of repair mortars have been designed and recommended for RC structures. Ordinary mortars (OMs), made of cement and boosted by different additives, are among the most frequently used repair mortars [13,14]. Additionally, polymer-modified cement (PMC) mortars [15] outperform OMs both mechanically and durably [16] ultra-high-performance (UHP) mortars [15] are expensive, and experience significant amount of spontaneous shrinkage; and engineered cementitious composite (ECC) mortars [11] have self-healing properties. Al these mortars, however, contain a substantial amount of cement, and thus are against low-carbon and sustainability notions of the contemporary construction industry. The cement production accounts for approximately 12–15% of the total energy used worldwide and 5–8% of the total carbon dioxide produced globally [17].

Alkali-activated mortar (AAM), also known as geopolymer mortar, is a more contemporary alternative for cement-based mortars and is made through reacting an alkali source with an aluminosilicate precursor with no cement [10] The favourable mechanical and durability properties of geopolymer binders make them extremely fit for repairing RC structures [15]. Geraldo et al. (2018) [10] studied the use of sodium hydroxide, silica fume, metakaolin, sand, and water, and [13] Teixeira et al., (2019) [13] investigated the performance of RC beams repaired by AAM and polymer mortar. Both studies reported that AAMs reach high strength in a short period of time and provide a high level of bonding with concrete substrate. Further, AAMs mechanically outperform polymer mortars [13]. The AAM-repaired beams exhibited greater deflections compared to control beams (undamaged beams), and the resulting bonding strength was found to be strong. However, excessive capillary absorption and efflorescence were observed for damp structural members because of the excessive presence of sodium [8].

1.3. Existing potential for more eco-friendly repair materials

Despite their mechanical advantages and being cement free, AAMs need a significant amount of natural aggregate, which can have adverse environmental impacts. Hence, researchers have begun to replace fine and coarse aggregates in concrete and mortars with waste industrial by-products like tyre rubber. This is because it reduces carbon dioxide and sulphur dioxide emissions, both of which are extremely rising [18,19] Scrap tyres are recycled to create a variety of products, including steel fibres, crumb rubbers, powder rubber, and even in rare cases, rubber fibres. The main contents of a tyre formulation are natural and synthetic rubbers, carbon black, metal, textile fabrics, etc [20]. Despite their great potential for use in concrete and mortar mixes, only 5% of recycled rubbers are used in the construction industry [21,22].

The replacement of fine and coarse aggregates with crumb rubber in concrete/mortar has both detrimental and beneficial effects. On the one hand, it reduces certain mechanical properties (e.g., compressive strength, flexural strength, tensile strength, and elastic modulus [17] and durability (e.g., moisture absorption and chloride ion permeability) of mortar, both of which restrict the use of rubber in structural elements. On the other hand, using rubber boosts ductility, energy dissipation and damping, thermal insulation, and acoustic properties of concrete/mortar [20,23–27] To increase the durability of rubberised concrete/mortar, researchers have studied the use of finer rubber particles such as fibre rubber and powder rubber. For instance, [30] Taha et al. (2008) [28] found that adding rubber powder to concrete improved its fracture characteristics, and [31] Gupta et al. (2019) [29] reported that using rubber fibres and powder increases concrete's resistance against chloride ions and raises its water permeability and carbonation depth. However, the appropriate replacement ratio of rubber particles in rubberised concrete/mortar should be determined through the correct balance between strength and durability depending on its application [28].

In a very recent study, based on the notion of the replacement of sand particles in AAMs with waste tire rubber, the authors conducted preliminary research on the development of a rubberised alkali-activated mortar (RAAM) for repairing concrete structures [30]. The studied RAAM contained no cement and uses waste tyre rubber (recycled resources), thus being more sustainable. It was found that the RAAM has a high potential for use in repairing concrete structures. Particularly, compatible mechanical properties and compatible failure modes between the control and repaired samples were observed, which are desirable features for repair purposes. However, low compressive and flexural strength values of the RAAM mixes were seen and also, the repaired beams were small-scale and unreinforced beam. Despite promising results, these pitfalls highlighted that the RAAM requires further investigation on its mix design as well as its application to large-scale RC beams. Therefore, this study will focus on the development and design of a suitable mix that boosts the RAAM's overall performance and provides high repair compatibility when applied to large-scale RC beams.

2. Experimental programme

In this study, a two-phase experimental programme is adopted to develop a RAAM for effective repair of RC beams. Hence, RAAM mixes as well as OM and AMM mixes are designed in the first phase through testing many small-scale samples. Then, a high-performance RAAM obtained from the first phase, AAM, and OM are used to repair and test damaged large-scale RC beams, thereby measuring the effectiveness of the RAAM in repair of concrete structures.

2.1. Mortar mix designs and tests

The proposed RAAM is composed of water (W), ground granulated blast-furnace slag (GGBS) as a binder, fine sand (FS), crumb rubber (CR), powder rubber (PR) as well as sodium hydroxide (SH) and sodium silicate (SS) as the main components of the AA solution. GGBS is the most typical component of AA-based mortars [31], a low-CO_2 substance, extremely vitreous and highly reactive with minimum variation [32]. Additionally, SH is the most extensively used activator in AA-based mortars because of its availability and low cost. It is typically mixed with SS to generate an alkaline solution and reach higher mechanical strength. Gomaa et al. (2017) [33] recommends the alkali ratio (SS/SH) and the binder ratio (W/GGBS) of respectively 1 and 0.4 to reach a high strength. Further, the amount of the rubber including both PR and CR, which replaces FS (replacement ratio), significantly affects the mortar's performance. Kianifar and Ahmadi (2023) [30] suggests the rubber ratio (PR/CR) of 0.5, given that they did not consider the segregation of the rubber particles as an influential factor.

2.1.1. Trial mortar mixes and tests

Despite the recommendations in the existing literature, due to the complexity of the RAAMs and lack of information about their design, three trial RAAM mixes are prepared as listed in Table 1. These trial mixes are studied to gain an insight into influential design factors of the RAAM prior to the main mix designs. The AA solution of these mixes contains 12 M SH and liquid SS of 40% purity (400 gr of SS dissolved in 1 L of water). The solution is prepared at least 24 hrs prior to the mortar production to ensure that it has been fully cooled off. The FS, CR, PR, and GGBS are thoroughly combined to reach a homogenous mix. Then, the solution is added to the mix, and the mixing process is continued for at least 4 mins to produce a well-mixed mortar.

To study the impact of curing method, the RAAM1 and RAAM2 are cured in an oven for 24 hrs at 70 °C, and then, is wrapped in cling film at an ambient temperature of 20 °C. On the contrary, the RAAM3 is cured at the room temperature and wrapped in cling film. For each of the RAAM1 and RAAM2 mixes, three 100 × 100 × 100 mm cubic samples are made (Fig. 1a) and tested in compression after the 3, 7, and 28 days of the curing (oven-cured samples), as shown in Fig. 1b. However, for

Table 1
Amounts of various contents per 1 m^3 of mortar for trial mixes.

Mix Name	GGBS (kg)	Agg/B	FS (kg)	CR (kg)	SH (kg)	W/GGBS	SS/SH	PR/CR	Replacement Ratio
RAAM1	666	1.55	867	34	96	0.40	1.30	0.50	0.15
RAAM2	666	1.55	691	62	96	0.40	0.83	0.50	0.30
RAAM3	666	1.55	691	62	96	0.40	1.00	0.50	0.30

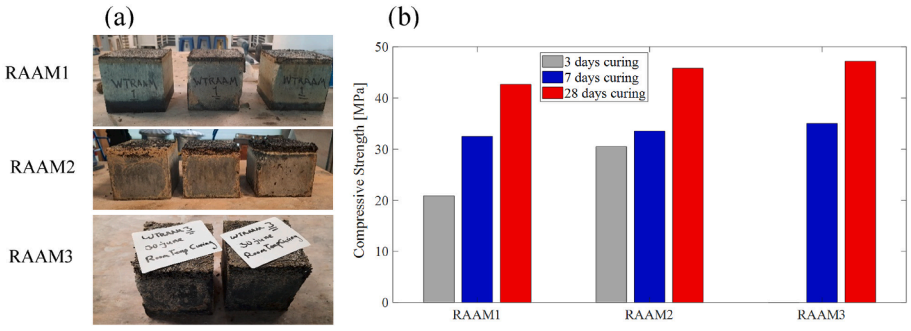

Fig. 1. (a) Trial samples, and (b) compressive strength test results.

the RAAM3, two samples are casted (Fig. 1a) and tested at the 7th day and 28th day of the curing (room temperature-cured samples).

As seen in Fig. 1a, the segregation occurs for all the samples. Particularly for the RAAM1 and RAAM2 (oven-cured samples), severe segregation between the rubber particles and other solid contents like GGBS and FS is seen. Therefore, the room temperature curing demonstrates superiority, and results in less segregation of the granular contents and consequently, less porosity. Further, the CR particles move to the top surface of the samples (a clear dark thick layer on the top is seen) due to their lower density (1100 kg/m^3), leading to significant segregation of the CR particles. Further, all the samples exhibit 28-day compressive strength values over 40 MPa (Fig. 1b).

To further investigate the segregation phenomenon and avoid it in design of the main mixes, a sieve analysis test is conducted to assess the gradation of the granular contents: FS, CR, and PR. The well-graded gradation curve minimises the voids between the granular particles, thereby reducing permeability and porosity and enhancing their compressive strength and durability [34]. The sieve analysis is performed according to ASTM C136 (2015) [35], where the Fuller Thompson curve is used as a benchmark for a well-graded mix [34]. Fig. 2a shows the gradation curves of the individual granular contents. It is seen in Fig. 2a that the FS particles are smaller than 2 mm and, neither CR nor PR contains any particle larger than 3 mm. This means that all the granular contents of the RAAMs are fine materials, and thus, achieving well-graded granular contents is impossible as seen in Fig. 2b. Thus, due to poorly graded granular contents (Fig. 2b) and the severe segregation observed (thick layer of CR on the top surface of the samples in Fig. 1a), the amount of the rubber ratio (PR/CR) will be increased up to 2 to ensure avoiding the segregation of particles.

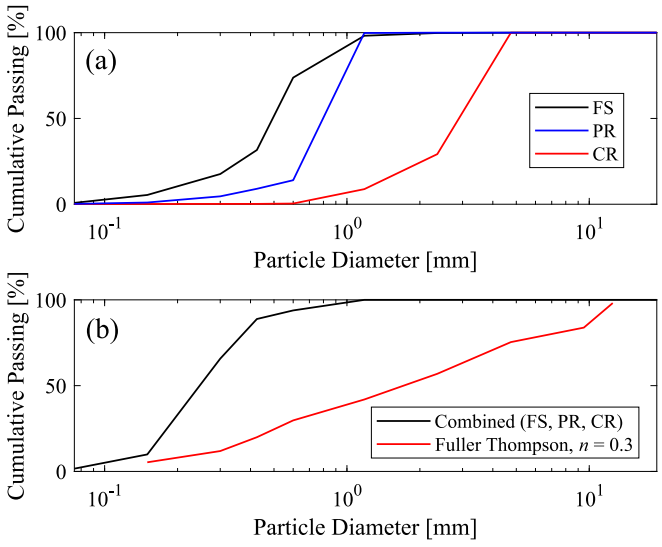

Fig. 2. Gradation curves for: (a) individual particles, and (b) combined particles.

2.1.2. Main mortar mixes and tests

To avoid the segregation phenomenon, the main RAMM mixes are designed for a high value of rubber ratio, PR/CR = 2, as shown in Table 2. Further, to assess the impact of the rubber content, RAAMs with replacement ratios of 0.15, 0.22, and 0.30 are developed. The binder ratio and alkali ratio are respectively taken 0.4 and 1 as recommended in [33]. The densities of the RAAM15, RAAM22, and RAAM30 are 2250 kg/m^3, 2180 kg/m^3, 2160 kg/m^3, respectively.

The OM with a water-to-cement ratio of 0.4 is designed for compressive strength of around 30 MPa, density of 2480 kg/m^3, and 2% air in its fresh form. The AAM is created using the same binder ratio, 0.4, and density of 2800 kg/m^3. The alkali ratio of the AAM is 1 with about 2% air in its fresh form.

A total of 105 main testing samples are manufactured and mechanically tested for compression, flexure, and bonding. For each mortar, three types of mechanical tests are conducted: (1) compressive strength according to ASTM C109 (2021) [36] (Fig. 3a), (2) flexural strength according to ASTM C293 (2010) [37] (Fig. 3b), and (3) bonding strength according to EN 1052–3 (2002) [38] (Fig. 4). For each mortar, fifteen 50 × 50 × 50 mm cubic samples are casted (Fig. 5a-5e), of which four samples are tested at the 3, 7, and 28 days of the room temperature curing, and three are tested at the 180th day. Six 40 × 40 × 160 mm samples are tested in flexure at the 28th day (Fig. 5f-5j).

For durability evaluation of the mortars, three cube samples of each mortar are tested for water absorption in accordance with ASTM C642 (2022) [39] after the 28th of curing. For each sample, the cling film is removed, the sample is dried, and its initial weight is measured. Afterwards, the sample is submerged in water for 0.5hrs and 48 hrs, and the weight is measured for each submersion period (e.g., 0.5 hrs and 48 hrs). The water absorption ratio for each submersion period is the relative change in the weight of the sample compared to the initial weight.

Another important feature of a repair is the quality of the bonding

Table 2
Amounts of various contents per 1 m^3 of mortar for main mixes.

Mix Name	Cement (kg)	GGBS (kg)	Agg/B	FS (kg)	CR (kg)	SH (kg)	Binder Ratio	SS/SH	PR/CR	Replacement Ratio
OM	650	–	2.42	1470	–	–	0.4	–	–	–
AAM	–	693	1.53	991	–	103.5	0.4	1	–	–
RAAM15	–	693	1.53	842	21	103.5	0.4	1	2	0.15
RAAM22	–	693	1.53	787	32	103.5	0.4	1	2	0.22
RAAM30	–	693	1.53	711	43	103.5	0.4	1	2	0.30

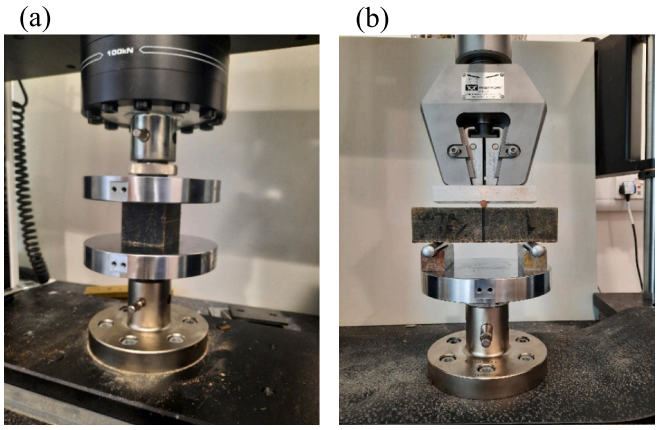

Fig. 3. Mortar mechanical tests: (a) compressive strength test, and (b) flexural strength test.

between the repair mortar and the concrete substrate. According to EN 1504-3 (2006) [40], the mortar must have a minimum bonding strength of 1.5 MPa for structural applications. The bonding of the concrete substrate-repair mortar interface is thus assessed through the triplet test method recommended in EN 1052-3 (2002) [38] (see Fig. 4). Three 40 × 40 × 160 mm prisms are bonded together by two layers of 10 mm mortars (Fig. 4a). The mortar interface is roughened, as is common in repair work, to increase the bonding. In the symmetric triplet test system, a load is applied to the middle of the concrete prisms to pass the shear force to the concrete-mortar interface at the joints, preventing the application of any eccentric loads, ([13], see Fig. 4c). Prior to the mortar application, each concrete prism is cured for 14 days in a water tank at an average temperature of 20° C. On the 28th day of the curing, the three samples of each mortar are tested for the bonding strength.

2.2. Large-scale RC beams and tests

From testing the RAAMs in section 2.1, the RAAM22 is selected as a high-performance repair material, which will be discussed in detail in section 3. Thus, three mortars (OM, AAM, and RAAM22) are used to repair three RC beams, with an undamaged RC beam (control beam) serving as a benchmark. Each beam has a rectangular cross section of 150 × 200 mm, a total length of 1500 mm, two 12 mm diameter longitudinal bars (yield strength of 500 MPa), and 200 mm-spaced 8 mm diameter shear links (see Fig. 6a). The control beam was designed to ensure flexural failure while providing sufficient shear resistance. The repair beams are damaged in the midspan where a cut as deep as the concrete cover, 25 mm, is made (Fig. 6a and 6b). The repair surface is wire brushed, chiselled, and submerged in water to provide a rough surface for better bonding prior to applying the repair mortars (Fig. 6c).

The concrete of the RC beams (concrete substrate) is designed for target compressive strength of 30 MPa at the 28th day of its curing in accordance with ACI 211.2.98 (1998) [41]. The concrete substrate's mix is 1: 2.6: 1.9, respectively for fine aggregate/cement, coarse aggregate/cement, and water/cement ratios. The beams are demoulded 24 hrs after casting, and then cured in a laboratory setting (temperature of 21 °C and relative humidity of 60%). To meet design specifications, superplasticizer is added to the fresh concrete to increase its workability, self-compacting capacity, and segregation resistance. The beams are cured for 28 days, then repaired by the mortars, and cured for 14 days prior to the flexural testing. All the RC beams are tested using a four-point bending testing machine in compliance with the ASTM C78 (2010) [42] (see Fig. 6b). The displacement-controlled approach is used to gradually apply the static load at a constant pace of 0.50 mm/min. An LVDT displacement sensor is placed at the midspan of the beams to measure their vertical displacement. One strain gauge is also installed at the midspan of the beam and the centre of the repair section (Fig. 6a). This strain gauge measures the strain at different levels of the vertical force.

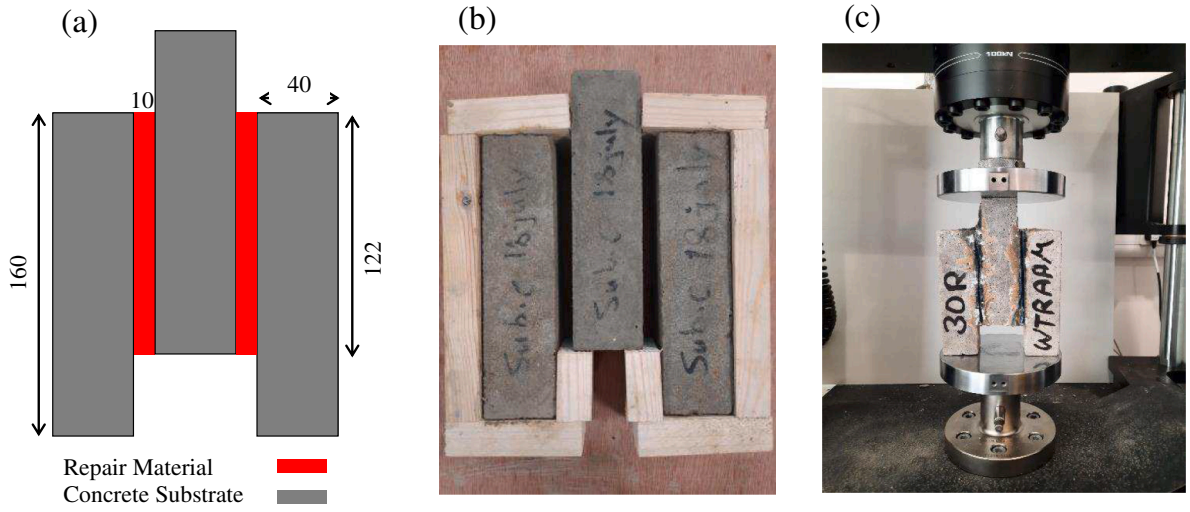

Fig. 4. Mortar bonding test: (a) dimensions in mm, (b) wooden mould for sample production, and (c) test setup.

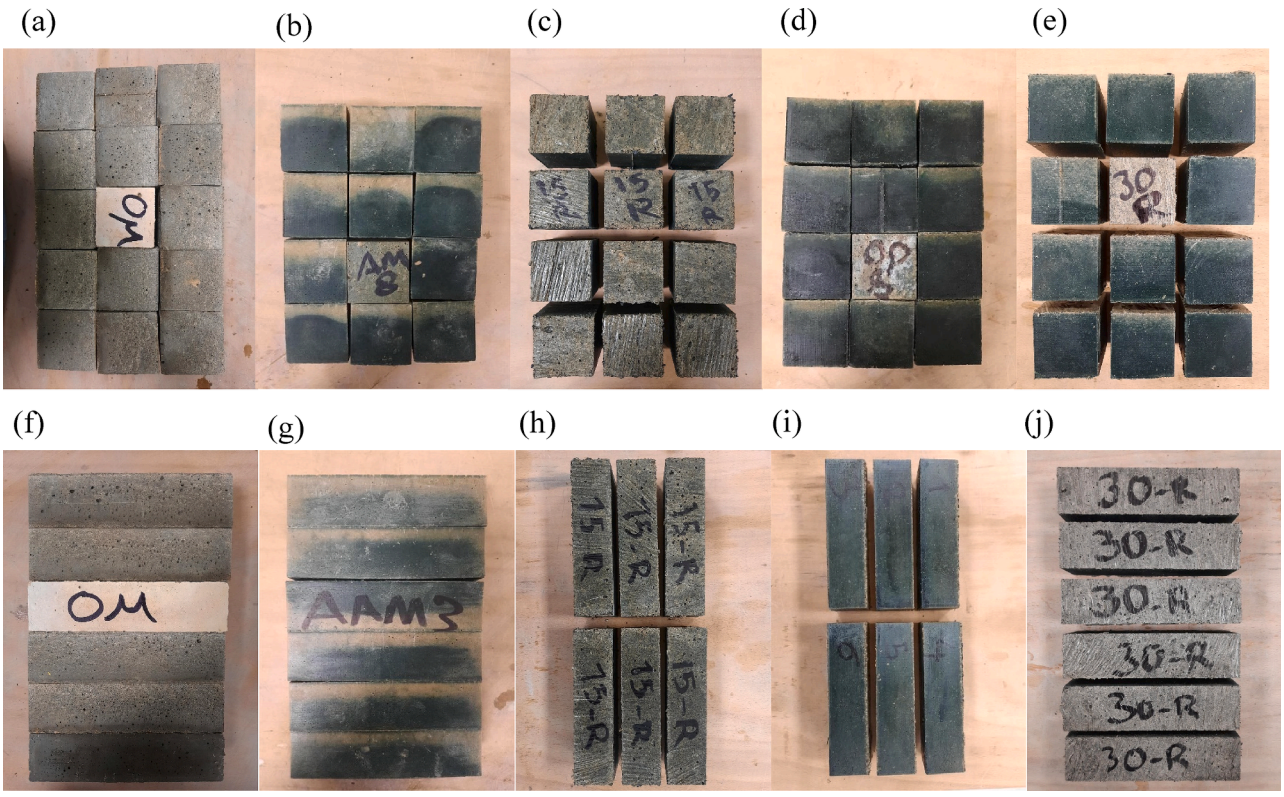

Fig. 5. Mortar samples for compressive strength test: (a) OM, (b) AAM, (c) RAMM15, (d) RAMM22, (e) RAMM30, and flexural strength test: (f) OM, (g) AAM, (h) RAAM15, (i) RAAM22, (j) RAAM30.

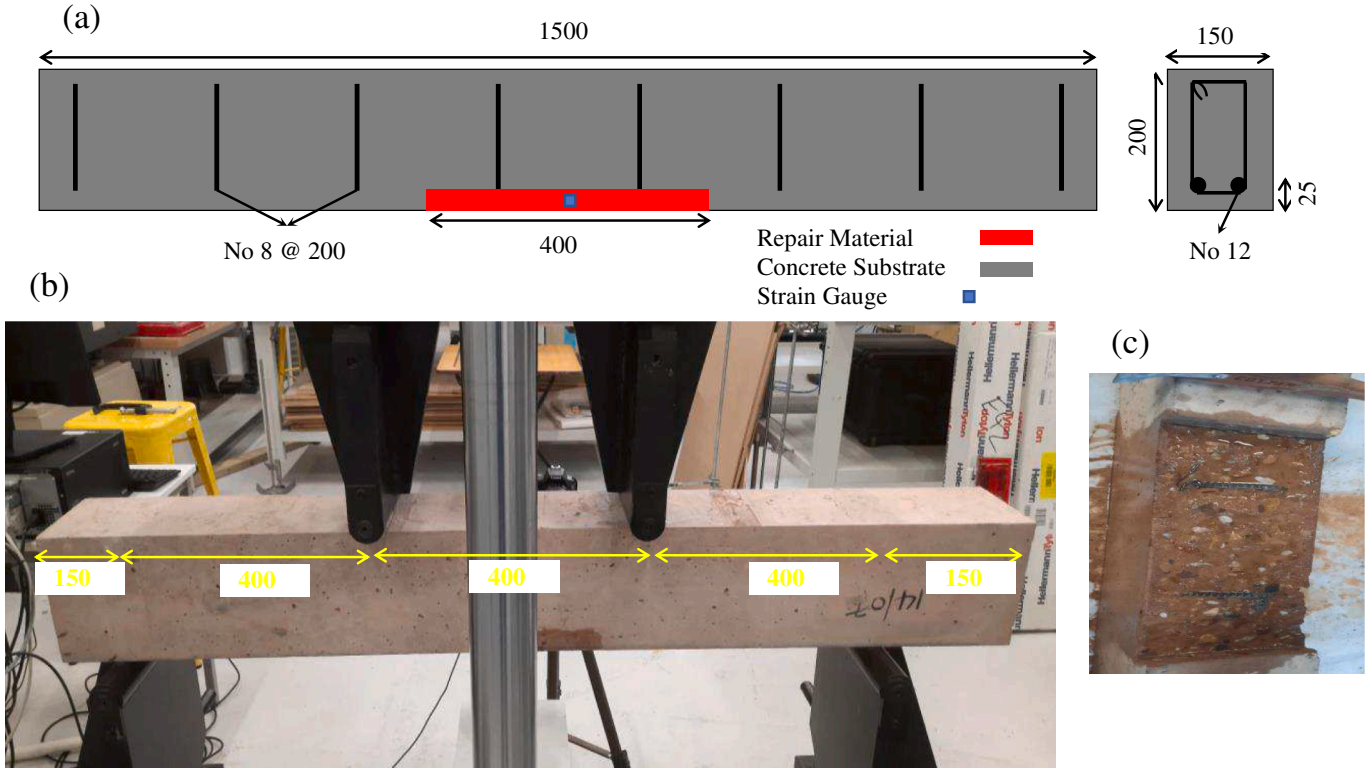

Fig. 6. (a) RC beams and repair dimensions, (b) four-point bending test setup, and (c) preparation of repair surface; note all dimensions are in mm.

3. Results and discussion

3.1. Mortar results

The substrate concrete-to-the repair mortar compressive strength ratio significantly affects the repair's performance in concrete beams [43]. Fig. 7a shows exemplary compressive stress–strain curves of the mortars at 3rd day of the curing. The AAM exhibits the highest compressive strength (maximum compressive stress for each stress–-strain curve) while the OM has compressive strength higher than the RAAM30, but less the RAAM15 and RAAM22. By filling voids and acting as a lubricant, rubber will operate as a filler material that can boost the overall density and the workability and application of the AAMs. Generally, adding rubber reduces mortar's compressive strength, and the RAAM22 shows 3-day compressive strength of around 34 MPa, slightly less than the RAAM15. However, the RAAM30 results in 3-day compressive strength of less than 25 MPa. The fracture stress of the mortars follows a trend similar to the compressive strength's. Further, the RAAM22 shows good compressive ductility, as large as the AAM, and far larger than the OM. Given both compressive strength and ductility features, the RAAM22 outperforms the RAA15 and RAAM30 (see Fig. 7a). Additionally, the AAM has a higher elastic modulus (initial slope of stress–strain curve), and adding rubber gradually reduces elastic modulus of the mortar. The use of rubber particles helps slow the spread of cracks by enhancing flexibility, dispersing tension, and absorbing strain. Fig. 7b illustrates the mean compressive strength of the mortars for the 3 days, 7 days, 28 days, and 180 days curing. The results are compatible with the discussion on the compressive strength in Fig. 7a. Interestingly, the AMM's mean compressive strength increases up to around 70 MPa after 180 days curing. The 180-day mean compressive strength values of the RAAM15, RAAM22, and RAAM30 are 65 MPa, 54 MPa, and 43 MPa, respectively.

Fig. 8a illustrates the mean flexural strength of the mortars. The OM shows the highest flexural strength. The AMM, RAAM15, and RAAM22 have very similar mean flexural strength and, a clear drop in the mean flexural strength is seen for the RAAM30. Fig. 8b shows exemplar shear stress–strain curves obtained from the bonding tests of the mortars. As seen, similar to compressive stress–strain curves of the mortars, the RAAM22 shows high shear strength and ductility compared to RAAM15 and RAAM30. It seems that high amount of rubber (RAAM30) reduces the mortar's shear strength, and thus leading to its failure before reaching higher ductility. Interestingly, the RAAM22 exhibits improved shear behaviour compared to the AAM.

The mean bonding (shear) strength is shown in Fig. 8c. As seen, adding rubber enhances the mean bonding strength of the AAM that is far higher than the OM. Specifically, the RAAM15 shows the highest mean bonding strength, and the RAAM22′s mean bonding strength is lower than the RAAM15′s, but noticeably larger than the rest of the mortars. Fig. 8d shows the mean results of the water absorption tests for the 0.5 hrs and 48 hrs submersions in water. The water absorption of the OM significantly increases from 3.6% to 7.3%. In contrast, there is no difference between the results of the 0.5 hrs and 48 hrs submersions for the AAM. Adding rubber increases water absorption rates [44]. Although this rise is not seen in the 0.5 hrs submersion tests, it is noticeable in the 48 hrs submersion test of the RAAMs. In comparison with the OM, the RAMMs have less water absorption capacity after 48 hrs of submersion, indicating that the RAAM absorbs less water for longer periods of time.

Fig. 9 shows the failure modes of the bonding samples. The failure modes of the mortars follow those reported in EN 1052–3 (2002) [38]. The RAAM samples fail by crushing, splitting, or shearing in the concrete substrate (Fig. 9c-9e), which is desirable for repair materials indicating strong bonding. On the contrary, the OM and AAM exhibit at least one shear failure in the bonding area due to weak bonding (Fig. 9a and 9b). Given all the influential features that determine overall performance of a repair material including compressive strength, flexural strength, bonding strength, compressive/shear ductility, and water absorption, the RAAM22 generally exhibits a high performance among all the RAAMs. Hence, the RAAM22 was selected together with the OM and AMM for the repair of the RC beams in section 2.2. Table 3 compares the amount of the embodied carbon footprint (in kg CO_2e) for the OM, AAM, and RAAM22, calculated according to Jones and Hammond, (2020) [45].The results clearly demonstrate that the AMM and RAAM22 have far lower embodied carbon compared to the OM, and hence, can highly increase the sustainability aspect of the repair mortars.

3.2. RC beams tests

Fig. 10 shows the crack pattern of the left half of the RC beams at failure state where the concrete at the top of the cross-section crushes under compression. The first cracks that appear during the testing are flexural cracks (vertical cracks) in the repair area for all the beams. Fig. 11a shows the force–displacement curves of all the beams. As listed in Table 2, the RAAM-repaired beam exhibits the largest cracking force (the force at which the first crack is observed), meaning that the cracking of the beam is significantly delayed when repaired by the RAAM. The reason can lie in the high ductility of the RAAM (see Fig. 7a and 8b). Both the RAAM- and AAM-repaired beams show slightly higher force capacity (maximum force from the force–displacement curve and reported in Table 4), and thus, slightly higher flexural strength values (see Table 4). Like the OM- and AAM-repaired beams, the RAAM-repaired beam shows a high maximum displacement before failure, leading to a high ductility index.

Fig. 11b shows the mortar strain versus applied force for the repaired beams. At a constant force, the WTRAA-repaired beam clearly exhibits a far smaller mortar strain, thus higher compatibility with the concrete substrate. The OM shows a very high strain at a very small force implying the strain incompatibility between the OM and the concrete substrate. The AAM shows a better performance exhibiting very small strain at around 5.7 kN. The RAAM starts experiencing high strain values at around 23.5 kN.

4. Conclusions

In this study, 105 small-scale samples were used to evaluate the effectiveness of a proposed rubberized alkali-activated mortar (RAAM)

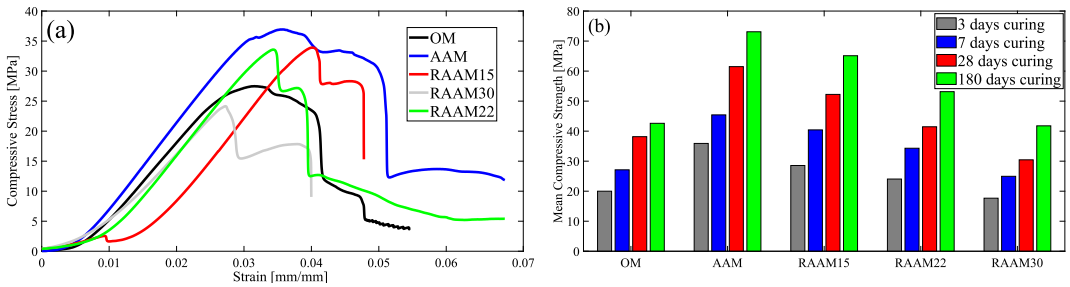

Fig. 7. (a) 3-day compressive stress–strain curve, and (b) mean compressive strength.

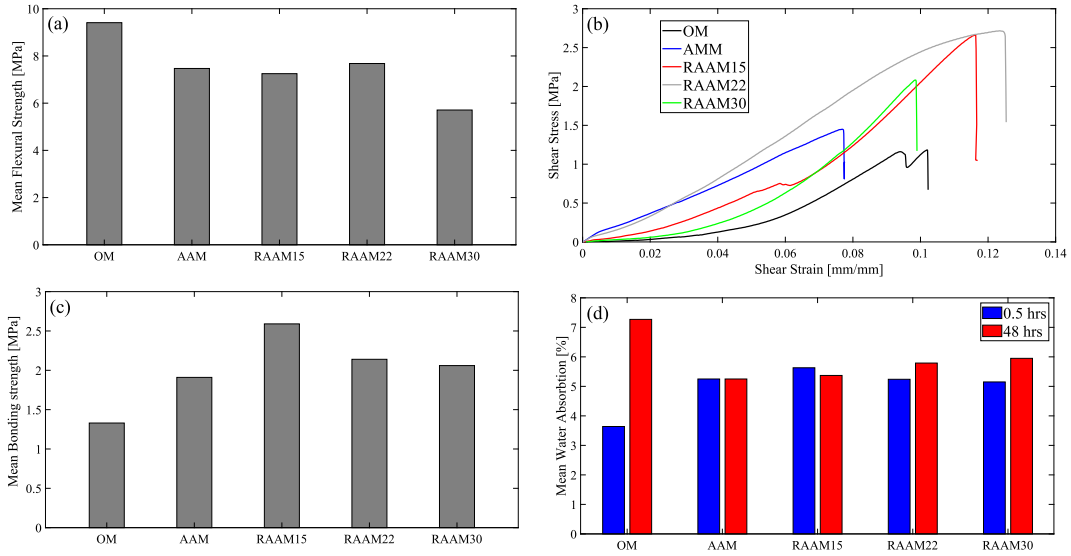

Fig. 8. (a) Mean flexural strength, (b) exemplar shear stress–strain curve, (c) mean bonding strength, and (d) water absorption results.

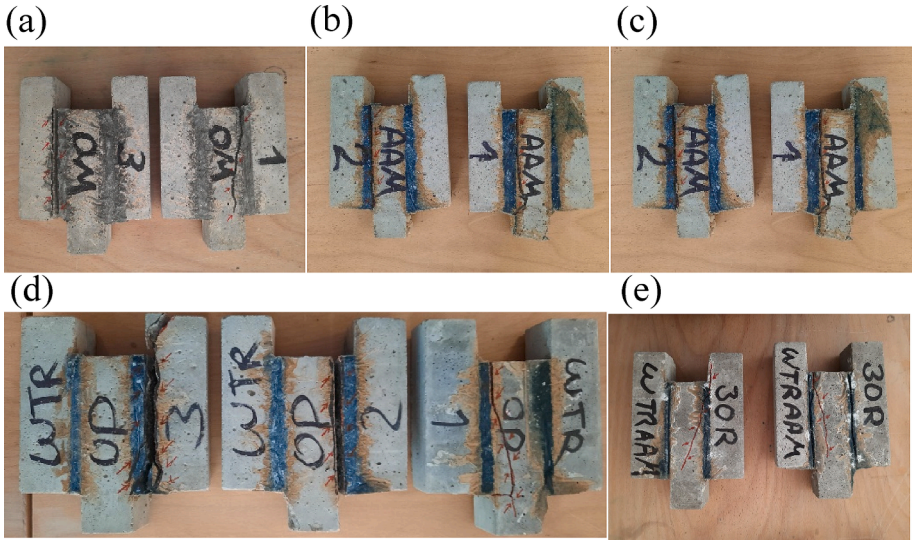

Fig. 9. Failure modes of the bonding samples: (a) OM, (b) AAM, (c) RAAM15, (d) RAAM22, and (e) RAAM30.

Table 3
Embodied carbon footprint of the mortars.

Contents	OM	AAM	RAAM22
Cement	519.7	0.0	0.0
GGBS	0.0	28.8	28.8
W	0.1	0.1	0.1
FS	11.0	7.4	6.6
kg CO_2e/m^3 mortar	530.8	36.3	35.5

for repairing damaged RC beams. Through a series of mechanical tests, including compressive, flexural, bonding strength, and water absorption, the performance of RAAM was compared to Ordinary (OM), and alkali activated (AAM) mortars. The results indicated that the RAAM with 22 % replacement of fine aggregates with rubber particles exhibited the most effective mix design for repairing damaged RC beams. Despite the general reduction in compressive strength caused by the addition of rubber, the RAAM22 mortar demonstrated a 3-day compressive strength of approximately 34 MPa. On the other hand, the OM mortar showed the highest flexural strength among the tested samples. Interestingly, the RAAM22 mortar displayed similar mean flexural strength to the AAM, suggesting its suitability for structural repairs. Additionally, the inclusion of rubber particles improved the bonding strength of the AAM, surpassing that of the OM mortar. Water absorption tests revealed that the RAAM absorbed less water over a longer period (48 hrs) compared to the OM mortar, indicating improved durability. Notably, RAAM22 production results in 15 times less embodied carbon footprint compared to OM and even slightly less than AAM, highlighting its sustainability.

During the 4-point bending tests conducted on RC repaired beams, the RAAM22-repaired beam exhibited cracking at a force of 35.8 kN, which was 46 % higher than the OM-repaired beam, and 28 % higher compared to the AAM-repaired RC beam. Furthermore, the RAAM22-repaired beam demonstrated higher force capacity (87 kN), flexural strength (17 MPa), and almost identical maximum displacement compared to the OM-repaired beam, indicating superior mechanical properties and ductility index. These findings underscore the promising potential of RAAM22 for the practical repair of RC concrete structures.

However, further research is necessary to assess the long-term durability, chemical penetration resistances, and microstructural

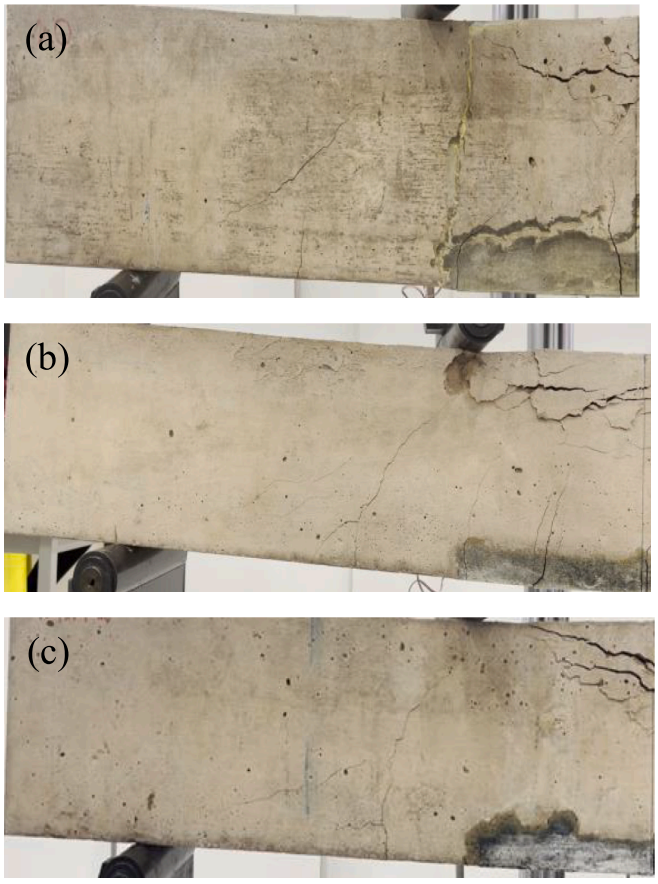

Fig. 10. Crack patterns of the beams at failure state (left half of the beam is shown): (a) OM-repaired, (b) AAM-repaired, and (c) RAAM-repaired.

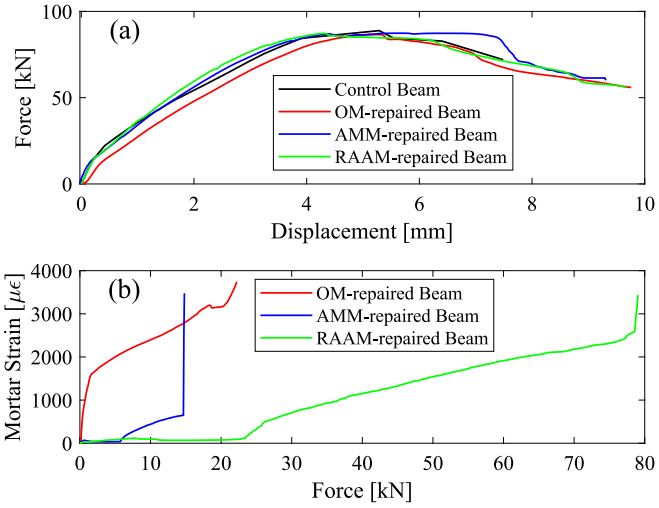

Fig. 11. Four-point bending testing of the RC beams: (a) force–displacement curves, and (b) mortar strain-force curves.

analysis of this mortar using advanced techniques such as Scanning Electron Microscope (SEM) or X-Ray Diffraction (XRD) before its implementation in engineering practice.

CRediT authorship contribution statement

Amin Zakeremamreza: Writing – original draft, Investigation. **Mohammad E. Kianifar:** Writing – review & editing, Supervision, Conceptualization. **Chidera Chibuisi:** Investigation. **Ehsan Ahmadi:** Writing – review & editing, Supervision, Methodology, Conceptualization. **Mohammad R. Salami:** Conceptualization, Supervision, Writing – review & editing.

Table 4
Critical values of the RC beams.

Beam Name	Cracking Force (kN)	Maximum Force (kN)	Maximum Displacement (mm)	Flexural Strength (MPa)
Control Beam	29.6	85.9	7.5	17.18
OM-repaired Beam	24.5	86.5	9.8	17.31
AAM-repaired Beam	28.0	87.3	9.3	17.47
RAAM-repaired Beam	35.8	87.2	9.7	17.45

Declaration of Competing Interest

The authors declare that they have no known competing financial interests or personal relationships that could have appeared to influence the work reported in this paper.

Data availability

Data will be made available on request.

Acknowledgement

The authors express their gratitude to the technical teams, resources, and funding provided by the engineering department of Birmingham City University that supported this research.

References

[1] R. Bahar, M. Benazzoug, S. Kenai, Performance of compacted cement-stabilised soil, Cem. Concr. Compos. 26 (2004) 811–820, https://doi.org/10.1016/j.cemconcomp.2004.01.003.
[2] A. Mukherjee, Recent Advances in Repair and Rehabilitation of RCC Structures with Nonmetallic Fibers Biopolymer soil stabilisation View project Guided wave based monitoring of bolted joints View project.
[3] M.Z. Jumaat, M.H. Kabir, M. Obaydullah, A Review of the Repair of Reinforced Concrete Beams. (2006).
[4] L.-Y. Xu, B.-T. Huang, V.C. Li, J.-G. Dai, High-strength high-ductility Engineered/Strain-Hardening Cementitious Composites (ECC/SHCC) incorporating geopolymer fine aggregates, Cem. Concr. Compos. 125 (2022) 104296.
[5] The Guardian: More than 3,200 UK bridges need repair, <https://www.theguardian.com/world/2022/mar/25/more-than-3200-uk-bridges-need-repair-local-authorities-say>.
[6] C. Moore, 4,000 of UK's busiest road bridges are in 'poor' condition.
[7] P. Duan, C. Yan, W. Luo, A novel waterproof, fast setting and high early strength repair material derived from metakaolin geopolymer, Constr. Build. Mater. 124 (2016) 69–73, https://doi.org/10.1016/j.conbuildmat.2016.07.058.
[8] S. Kramar, A. Šajna, V. Ducman, Assessment of alkali activated mortars based on different precursors with regard to their suitability for concrete repair, Constr. Build. Mater. 124 (2016) 937–944, https://doi.org/10.1016/j.conbuildmat.2016.08.018.
[9] S.U. Al-Dulaijan, M.M. Al-Zahrani, H. Saricimen, M. Maslehuddin, M. Shameem, T. A. Abbasi, Effect of rebar cleanliness and repair materials on reinforcement corrosion and flexural strength of repaired concrete beams.
[10] R.H. Geraldo, O.G. Teixeira, S.R.C. Matos, F.G.S. Silva, J.P. Gonçalves, G. Camarini, Study of alkali-activated mortar used as conventional repair in reinforced concrete, Constr. Build. Mater. 165 (2018) 914–919, https://doi.org/10.1016/j.conbuildmat.2018.01.063.
[11] J. Shao, H. Zhu, X. Zuo, W. Lei, S.M. Borito, J. Liang, F. Duan, Effect of waste rubber particles on the mechanical performance and deformation properties of epoxy concrete for repair, Constr. Build. Mater. 241 (2020) 118008.
[12] M. Sánchez, P. Faria, L. Ferrara, E. Horszczaruk, H.M. Jonkers, A. Kwiecień, J. Mosa, A. Peled, A.S. Pereira, D. Snoeck, M. Stefanidou, T. Stryszewska, B. Zając,

External treatments for the preventive repair of existing constructions: a review, Constr. Build. Mater. 193 (2018) 435–452.
[13] O.G. Teixeira, R.H. Geraldo, F.G. da Silva, J.P. Gonçalves, G. Camarini, Mortar type influence on mechanical performance of repaired reinforced concrete beams, Constr. Build. Mater. 217 (2019) 372–383, https://doi.org/10.1016/j.conbuildmat.2019.05.035.
[14] C. Fapohunda, B. Akinbile, A. Shittu, Structure and properties of mortar and concrete with rice husk ash as partial replacement of ordinary Portland cement – a review, Int. J. Sustain. Built Environ. 6 (2) (2017) 675–692.
[15] Y.-S. Wang, K.-D. Peng, Y. Alrefaei, J.-G. Dai, The bond between geopolymer repair mortars and OPC concrete substrate: strength and microscopic interactions, Cem. Concr. Compos. 119 (2021) 103991.
[16] S.K. Park, D.S. Yang, Flexural behavior of reinforced concrete beams with cementitious repair materials, Mater. Struct./Materiaux et Constructions 38 (2005) 329–334, https://doi.org/10.1617/14051.
[17] A.M. Rashad, D.M. Sadek, Behavior of alkali-activated slag pastes blended with waste rubber powder under the effect of freeze/thaw cycles and severe sulfate attack, Constr. Build. Mater. 265 (2020) 120716.
[18] S. Gwon, Y. Jeong, J.E. Oh, M. Shin, Sustainable sulfur composites with enhanced strength and lightweightness using waste rubber and fly ash, Constr. Build. Mater. 135 (2017) 650–664, https://doi.org/10.1016/j.conbuildmat.2017.01.024.
[19] F. Wang, X. Ping, J. Zhou, T. Kang, Effects of crumb rubber on the frost resistance of cement-soil, Constr. Build. Mater. 223 (2019) 120–132, https://doi.org/10.1016/j.conbuildmat.2019.06.208.
[20] A. Fazli, D. Rodrigue, Recycling waste tires into ground tire rubber, J. Compos. Sci. 4 (3) (2020) 103.
[21] D. Lo Presti, Recycled tyre rubber modified bitumens for road asphalt mixtures: a literature review, Constr. Build. Mater. 49 (2013) 863–881.
[22] F. Aslani, Mechanical properties of waste tire rubber concrete, J. Mater. Civ. Eng. 28 (2016), https://doi.org/10.1061/(asce)mt.1943-5533.0001429.
[23] N.M. Miller, F.M. Tehrani, Mechanical properties of rubberized lightweight aggregate concrete, Constr. Build. Mater. 147 (2017) 264–271, https://doi.org/10.1016/j.conbuildmat.2017.04.155.
[24] G. Girskas, D. Nagrockienė, Crushed rubber waste impact of concrete basic properties, Constr. Build. Mater. 140 (2017) 36–42, https://doi.org/10.1016/j.conbuildmat.2017.02.107.
[25] K. Bisht, P.V. Ramana, Evaluation of mechanical and durability properties of crumb rubber concrete, Constr. Build. Mater. 155 (2017) 811–817, https://doi.org/10.1016/j.conbuildmat.2017.08.131.
[26] A.S.M. Mendis, S. Al-Deen, M. Ashraf, Flexural shear behaviour of reinforced Crumbed Rubber Concrete beam, Constr. Build. Mater. 166 (2018) 779–791, https://doi.org/10.1016/j.conbuildmat.2018.01.150.
[27] K. Strukar, T. Kalman Šipoš, I. Miličević, R. Bušić, Potential use of rubber as aggregate in structural reinforced concrete element – a review, Eng. Struct. 188 (2019) 452–468.
[28] M.M. Reda Taha, M. Asce, A.S. El-Dieb, M.A. Abd El-Wahab, M.E. Abdel-Hameed, Mechanical, Fracture, and Microstructural Investigations of Rubber Concrete. doi: 10.1061/ASCE0899-1561200820:10640.
[29] T. Gupta, S. Siddique, R.K. Sharma, S. Chaudhary, Behaviour of waste rubber powder and hybrid rubber concrete in aggressive environment, Constr. Build. Mater. 217 (2019) 283–291, https://doi.org/10.1016/j.conbuildmat.2019.05.080.
[30] M.E. Kianifar, E. Ahmadi, kianifar, ahmadi, Int. J. Struct. Constr. Eng. 17 (2023) 68–74.
[31] D.W. Law, A.A. Adam, T.K. Molyneaux, I. Patnaikuni, Durability assessment of alkali activated slag (AAS) concrete, Materials and Structures/Materiaux et Constructions 45 (2012) 1425–1437, https://doi.org/10.1617/s11527-012-9842-1.
[32] J. Osio-Norgaard, J.P. Gevaudan, W.V. Srubar, A review of chloride transport in alkali-activated cement paste, mortar, and concrete, (2018).
[33] E. Gomaa, S. Sargon, C. Kashosi, M. ElGawady, Fresh properties and compressive strength of high calcium alkali activated fly ash mortar, J. King Saud Univ. – Eng. Sci. 29 (2017) 356–364, https://doi.org/10.1016/j.jksues.2017.06.001.
[34] Y. Weng, M. Li, M.J. Tan, S. Qian, Design 3D printing cementitious materials via Fuller Thompson theory and Marson-Percy model, Constr. Build. Mater. 163 (2018) 600–610, https://doi.org/10.1016/j.conbuildmat.2017.12.112.
[35] ASTM C136: Standard Test Method for Sieve Analysis of Fine and Coarse Aggregates.
[36] ASTM C109: Standard test method for compressive strength of hydraulic cement mortars (using 2-in. or [50 mm] cube specimens).
[37] ASTM C293: Standard Test Method for Flexural Strength of Concrete (Using Simple Beam With Center-Point Loading).
[38] EN 1052-3: Methods of test for masonry : Part 3 : determination of initial shear strength. British Standards Institution (2002).
[39] ASTM C642: Standard Test Method for Density, Absorption, and Voids in Hardened Concrete. ASTM international. 21, 1–3 (2022).
[40] EN 1504-3: Products and systems for the protection and repair of concrete structures - Definitions, requirements, quality control and evaluation of conformity - Part 3: Structural and non-structural repair. (2006).
[41] ACI 211.2.98: ACI 211.2.98. (1998).
[42] ASTM C78: Standard Test Method for Flexural Strength of Concrete (Using Simple Beam with Third-Point Loading).
[43] R.R. Pattnaik, P.R. Rangaraju, Investigation on flexure test of composite beam of repair materials and substrate concrete for durable repair, J. Inst. Eng. (India): Series A 95 (2014) 203–209, https://doi.org/10.1007/s40030-014-0096-5.
[44] F. Ameri, P. Shoaei, H. Reza Musaeei, S. Alireza Zareei, C.B. Cheah, Partial replacement of copper slag with treated crumb rubber aggregates in alkali-activated slag mortar, Constr. Build. Mater. 256 (2020) 119468.
[45] D.C. Jones, P.G. Hammond, Concrete embodied carbon footprint calculator, https://circularecology.com/concrete-embodied-carbon-footprint-calculator.html.